LETTER

doi:10.1038/nature14648

The role of ridges in the formation and longevity of flat slabs

Sanja Knezevic Antonijevic[1], Lara S. Wagner[2], Abhash Kumar[1], Susan L. Beck[3], Maureen D. Long[4], George Zandt[3], Hernando Tavera[5] & Cristobal Condori[5]

Flat-slab subduction occurs when the descending plate becomes horizontal at some depth before resuming its descent into the mantle. It is often proposed as a mechanism for the uplifting of deep crustal rocks ('thick-skinned' deformation) far from plate boundaries, and for causing unusual patterns of volcanism, as far back as the Proterozoic eon[1]. For example, the formation of the expansive Rocky Mountains and the subsequent voluminous volcanism across much of the western USA has been attributed to a broad region of flat-slab subduction beneath North America that occurred during the Laramide orogeny (80–55 million years ago)[2]. Here we study the largest modern flat slab, located in Peru, to better understand the processes controlling the formation and extent of flat slabs. We present new data that indicate that the subducting Nazca Ridge is necessary for the development and continued support of the horizontal plate at a depth of about 90 kilometres. By combining constraints from Rayleigh wave phase velocities with improved earthquake locations, we find that the flat slab is shallowest along the ridge, while to the northwest of the ridge, the slab is sagging, tearing, and re-initiating normal subduction. On the basis of our observations, we propose a conceptual model for the temporal evolution of the Peruvian flat slab in which the flat slab forms because of the combined effects of trench retreat along the Peruvian plate boundary, suction, and ridge subduction. We find that while the ridge is necessary but not sufficient for the formation of the flat slab, its removal is sufficient for the flat slab to fail. This provides new constraints on our understanding of the processes controlling the beginning and end of the Laramide orogeny and other putative episodes of flat-slab subduction.

Oceanic plates subduct at different angles ranging from steep to shallow, with flat slabs representing the horizontal endmember. The subduction of buoyant aseismic ridges and plateaus comprising overthickened oceanic crust has long been thought to play a part in the formation of flat slabs[3]. More recent work has identified other potential contributing factors, including trench retreat[4,5], rapid overriding plate motion[4,5], and suction between the flat slab and overriding continental mantle lithosphere[5]. Many of these studies do not preclude the need for additional buoyancy from overthickened oceanic crust. However, a few recent studies suggest that subducting ridges do not affect the formation or sustainability of flat slabs[6,7].

To evaluate the influence of subducting ridges on the evolution of flat slabs, we focus on the flat slab in southern Peru (Fig. 1). Here, the subducting Nazca Ridge trends at an oblique angle to relative plate motion, resulting in a northward migration of the overriding continent relative to the down-going ridge[8]. We have collected and analysed data from two deployments of broadband seismometers in central and southern Peru: PULSE (Peru Lithosphere and Slab Experiment)[9], and CAUGHT (Central Andean Uplift and Geodynamics of High Topography)[10]. We also incorporate data from eight stations from the PERUSE deployment (Peru Slab Experiment)[11] and the permanent station called NNA in Lima, Peru (Fig. 1). Here we present a three-dimensional model of shear-wave velocity structure between −10° and −18°, obtained from the inversion of earthquake-generated Rayleigh-wave-phase velocities (Fig. 2 and Extended Data Figs 2–10). We also relocate slab seismicity across our study area using a double difference methodology (Figs 2 and 3, Extended Data Fig. 1 and Supplementary Table 1) (see Methods for details).

Our tomographic images and improved earthquake locations show the flat slab to be shallowest along the present-day projected location of the subducted Nazca Ridge (Figs 2g and 3g, h). To the south (Fig. 2h), the slab transitions abruptly from flat to normal, and earthquake locations align with an increase in shear-wave velocity in our model. To the north, where previous studies have proposed a broad flat slab of relatively uniform depth[12,13], we see a gradual but marked deepening of the plane of seismicity associated with subducted slab known as the Wadati–Benioff zone (Figs 2e, f and 3g, h). To the east, high shear-wave velocities associated with the flat slab extend substantially inboard (that is, away from the trench, inland) than the seismically active portion of the plate (Figs 2g and 3g,h). The downward bend

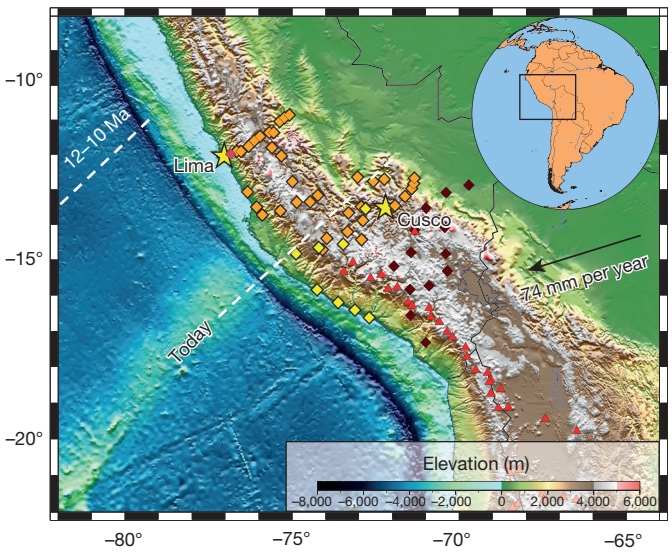

Figure 1 | Reference map of the Peruvian flat-slab region, illustrating the subducting Nazca Ridge beneath the advancing South American plate. Diamonds represent seismic stations used in this study: orange, PULSE; dark red, CAUGHT; yellow, PERUSE; red, the permanent NNA station. Yellow stars represent the cities Lima and Cusco. Red triangles represent volcanoes active during the Holocene epoch. The black arrow indicates the relative motion of the South American plate with respect to the Nazca Plate[21]. Dotted white lines show the estimated position of the Nazca Ridge 12–10 Ma and today[8].

[1]Department of Geological Sciences, University of North Carolina at Chapel Hill, CB 3315, Chapel Hill, North Carolina 27599, USA. [2]Department of Terrestrial Magnetism, Carnegie Institution for Science, 5241 Broad Branch Road NW, Washington DC 20015, USA. [3]Department of Geosciences, University of Arizona, 1040 East 4th Street, Tucson, Arizona 85721, USA. [4]Department of Geology and Geophysics, Yale University, 210 Whitney Avenue, New Haven, Connecticut 06511, USA. [5]Instituto Geofísico del Perú, Calle Badajoz 169, Lima 15012, Peru.

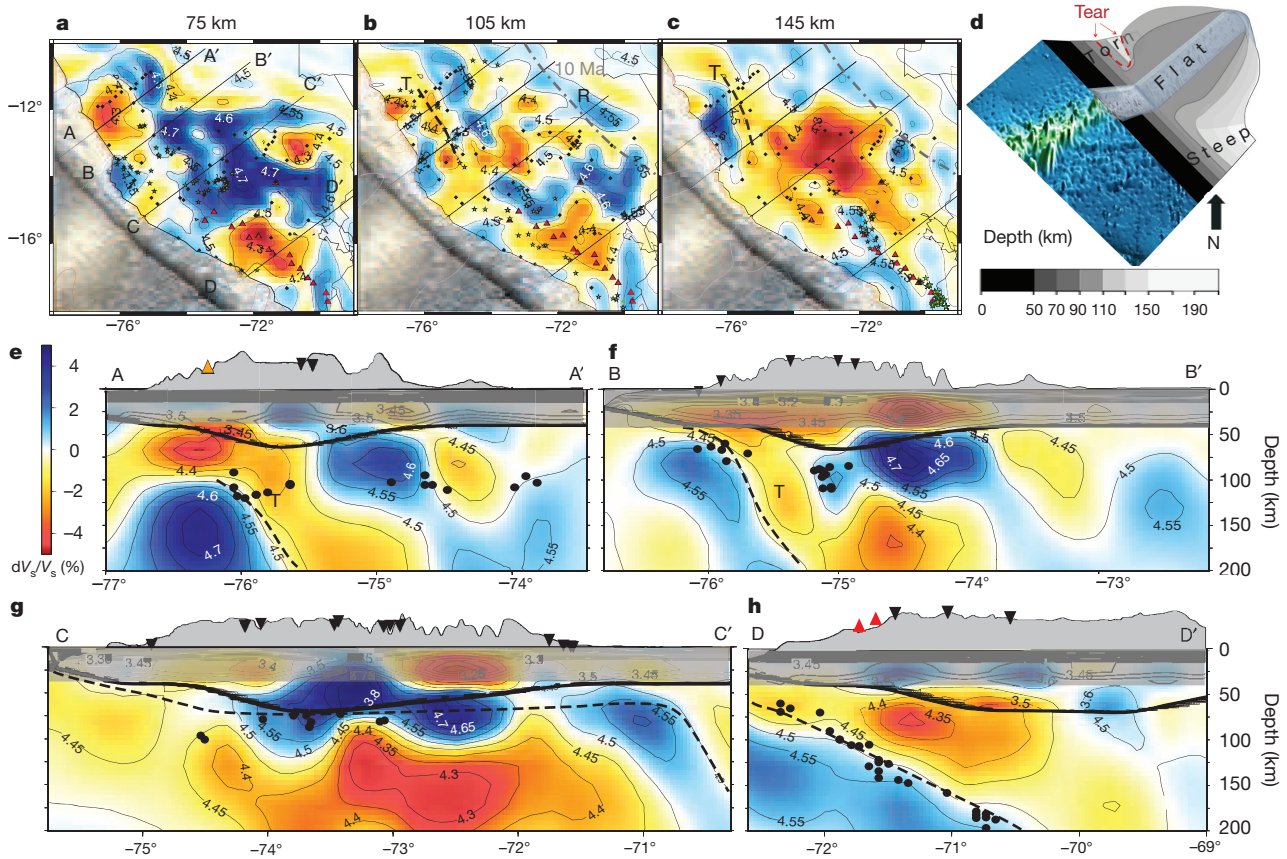

Figure 2 | Three-dimensional model of the structure of shear-wave velocities between −10° and −18°. **a**–**c**, Shear-wave velocities and seismicity at depths of 75 km (**a**), 105 km (**b**) and 145 km (**c**), and transects along the northern reinitiating steep slab (A–A′, B–B′), flat slab (C–C′) and southern steep slab (D–D′) segments. Colours indicate velocity deviations, dV_s/V_s (%); contours show absolute velocities in kilometres per second (numbered). **a**–**c**, Black circles represent stations used in our study; red triangles are Holocene volcanoes; green stars are earthquakes within 20 km of the depth shown; black lines refer to cross-sections shown in **e**–**h**. The grey dashed line in **b** and **c** shows the location of the trench 10 Ma (ref. 8); the black dashed line (labelled 'T') indicates the location of the slab tear. 'R' refers to the resumption of steep subduction at the eastern edge of the flat slab. **d**, Inferred flat-slab geometry along the Nazca Ridge track, and slab tear north of the ridge. **e**–**h**, Cross-sections of slab segments shown in **a**–**c**. Black dots show earthquake locations from this study; black inverted triangles are stations; red triangles are Holocene volcanoes; orange triangle represents the location of a measurement of unusually high heat flow[15]. Dashed lines show the inferred top of the slab. The thick black line shows the crustal thickness.

in the high-velocity plate at the easternmost extent of the flat slab appears to coincide with the location of the Peruvian trench about 10 million years ago (Ma)[8].

Of particular note is the geometry of the subducted plate north of the projected Nazca Ridge track (Fig. 2a–c, e, f). Here, we observe a dipping high-velocity anomaly to the trenchward side of a dipping low-velocity anomaly. We note the similarity between these structures (in an area previously believed to comprise typical flat slab) and those observed to the south beneath the active arc (Fig. 2e, f, h). We also note the difference between these structures and those adjacent to the ridge, where the continuous flat slab is well resolved (Fig. 2e–g and Extended Data Figs 3, 6–10). We interpret the westward-dipping low-velocity region parallel to the trench to be evidence of asthenosphere (the viscous, weak region of the upper mantle) between two torn portions of subducted plate. The dipping high-velocity anomaly to the west indicates the presence of a normally dipping slab extending to a depth of at least 200 km. This is consistent with the location of shear-wave scatterers identified from converted phases in earlier studies[14]. We propose that the subhorizontal seismicity to the east of the tear is located in remnant flat slab that has not yet been fully subducted. Local shear wave splitting studies show that shear waves move faster parallel to the trench[9], consistent with north–south-directed asthenospheric flow through a break in the Nazca plate. We also note the presence of a localized high heat flow (196 mW s^{-2}) above this low-velocity anomaly[15] (Fig. 2e). Along the northernmost transect, the location of the slab is not well resolved above a depth of about 100 km (Fig. 2e). Future work using ambient noise tomography may help us to resolve the slab geometry here, by providing improved constraints on velocities at shallower depths.

We incorporate the results of previous geodynamic modelling studies with our results, to create a conceptual model of the temporal evolution of the Peruvian flat slab (Fig. 3). We begin with the initiation of ridge subduction at approximately 11.2 Ma (ref. 8), before which we assume normal subduction across our study area (Fig. 3a). From there, we base our proposed temporal evolution of the Peruvian flat slab on four principles.

First, we present our conceptual model from the reference frame of a laterally stationary Nazca plate. Second, while most of the Nazca plate sinks vertically at a relatively constant rate, the plate containing the Nazca Ridge ceases to sink at a depth of about 90 km (Fig. 3b–f). We propose that this is due to buoyancy imparted by the overthickened oceanic crust and harzburgite layer associated with the ridge, consistent with previous modelling studies[16]. Third, we observe that the modern inboard extent of the Peruvian flat slab corresponds to the location of the trench at about 10 Ma. Given that the projected location of the Nazca Ridge extends further to the east, this finding suggests that

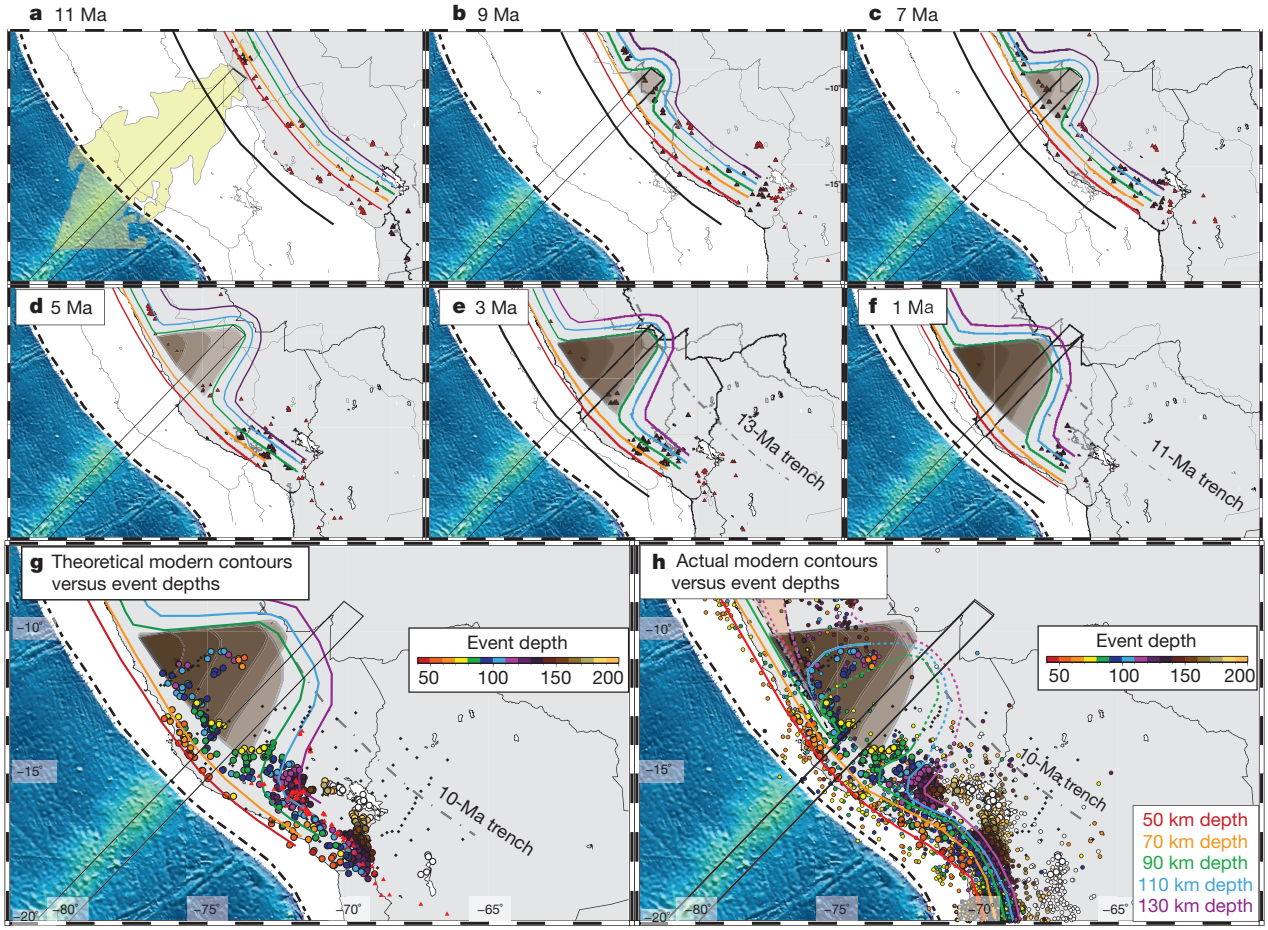

Figure 3 | Proposed evolution of the Peruvian flat slab. **a**–**f**, Proposed contours of the subducted slab, assuming that the ridge remains buoyant for 10 Ma after entering the trench. The approximate location of the subducted ridge is denoted by the black rectangular outline. Brown areas show areas of the continent underlain by flat slab at each time step. Triangles indicate volcanoes active during the 2 Myr following the time of the frame shown[22]. The location of the South American continent relative to the Nazca Ridge follows ref. 8. In **a**, we show the location of the projection of the mirror image of the Nazca Ridge (in yellow) that formed synchronously with the Nazca Ridge on the Pacific Plate when these plates were first created at the spreading centre following ref. 8. In **e**, red triangles show volcanism from 3 Ma to 2 Ma, and brown triangles show volcanism from 2 Ma to 1 Ma. In **f**, volcanism is shown for 1 Ma to 0 Ma (not including Holocene volcanism). **g**, Modern seismicity from this study (large circles) with depths >50 km, and contours as they would be if the removal of the ridge did not affect the longevity of the flat slab. **h**, Modern seismicity from this study and local seismicity at depth >50 km, as reported in the ISC catalogue for years 2004–2014, shown as smaller circles[17]. We plot our observed slab contours on the basis of our earthquake locations and the location of high-velocity anomalies in our tomographic results. Dashed lines indicate contours that are less certain, either because of a paucity of earthquakes or because they lie outside of our region of good tomographic resolution. The pink triangular shape shows the region with very limited seismicity that may indicate a slab window caused by tearing and the reinitiation of normal subduction.

some portion of the Nazca Ridge has resumed normal subduction. We propose that, over time, the kinetically slow conversion of basalt and gabbro to eclogite in the overthickened crust of the Nazca Ridge results in an increase in the density of the horizontal plate. Given the inboard extent of the modern flat slab, we propose that, approximately 10 Ma after entering the trench, the overthickened oceanic crust of the Nazca Ridge becomes sufficiently eclogitized that it is no longer neutrally buoyant and therefore resumes its vertical descent (Figs 2b, g and 3e–g).

Finally, modelling studies indicate that suction between the horizontal plate and overriding continental lithosphere hinders the removal of the flat slab[5]. In our study area, this is important because the portion of the continent under which the flat slab initially forms moves northwest relative to the ridge over time. To test whether the flat slab will perpetuate beneath these continental regions after the departure of the ridge, we apply the fourth principle to our model: continental regions previously underlain by the flat slab will continue to have flat slab beneath them for some time (brown regions in Fig. 3). This results in a broadening of the flat slab as new continental areas to the south become underlain by the ridge and associated flat slab, while areas to the north that were previously underlain by the ridge maintain their flat-slab geometry. This is consistent with earlier studies that attribute the along-strike (trench parallel) extent of the Peruvian flat slab to the southward sweep of the Nazca Ridge over time[8,9].

The proposed temporal evolution of the Peruvian flat slab shown in Fig. 3 combines the influences of trench retreat/overriding plate motion, suction, and ridge buoyancy. It assumes that the combination of all three forces is necessary for the formation of the flat slab, but that the first two are sufficient to perpetuate the flat slab after the departure of the ridge. A comparison between our conceptual model's slab geometry at present (Fig. 3g) with actual (observed) slab geometry (Fig. 3h) allows us to test these assumptions. The abrupt edge of the flat slab that we observe south of the ridge is very similar to that proposed by our conceptual model. We note that the dominant principle controlling the geometry of the flat slab here is the effect of ridge buoyancy, as there is no difference in trench rollback or continental lithospheric structure that might affect suction along strike in this region. Our observations therefore support the necessary contribution of the ridge to the formation of flat slabs, but are

also not inconsistent with additional contributions from suction and trench rollback.

Differences between the observed slab geometry and the geometry derived from our conceptual model are visible to the north of the ridge. In this area, the effect of the ridge is no longer present, and the geometry of the flat slab in our conceptual model is controlled by the effects of suction and trench rollback alone. Although both our conceptual model and our observations indicate a flat slab that broadens to the northwest of the ridge, the detailed morphologies are very different. In addition to an overall deepening of the flat slab north of the ridge (Fig. 3g, h and Extended Data Fig. 1), we observe a clear trench-parallel break in the subducted plate and a resumption of normal subduction trenchward of this tear (Figs 2a–c and 3h). This strongly suggests that, despite the presence of suction and trench rollback, the flat slab is no longer stable once the buoyant Nazca Ridge has been removed. Furthermore, once a break is present, the newly subducted plate assumes a normal steep dip angle, rather than a flat-slab geometry. In this study we are not able to resolve the northern extent of the Peruvian flat slab, nor can we establish the along-strike extent of the tear. However, International Seismological Centre Catalog locations north of our study area show a gap in seismicity that may be consistent with the absence of a flat slab because of a progressively tearing plate (Fig. 3h)[17]. The northward extent of the flat slab east of the tear may be due in part to the subduction of the Inca Plateau[8], although this is beyond the scope of our study.

Our model is applicable to all flat-slab geometries in cases for which a distinct change of dip angle is observed. This change in dip occurs at the depth at which the slab becomes neutrally buoyant. Our results may not be applicable to slabs when the dip angle is constant but very shallow[7] (for example, in Alaska and in the Cascadia region of the USA). Slabs that dip at a shallow angle sink at a constant rate, which is inconsistent with a period of neutral buoyancy. Such slabs may have effects that are similar to those produced by flat slabs, although they do not result in a complete cessation of arc volcanism (as occurred during the Laramide orogeny and is observed in Peru today), only its inboard deflection.

Our results may provide insights into the final stages of flat-slab subduction. Previous studies used volcanic patterns to reconstruct the formation and foundering of the Farallon flat slab in the western USA[2,18,19]. The diversity of models for the progression of this foundering is indicative of the insufficiency of the constraints provided by volcanic trends alone. Our results suggest that once the flat slab extends some distance away from the buoyant feature, it will begin to sink and/or tear. Tearing of the Farallon plate caused by an excessively wide flat slab may be consistent with tomographic images of broken fragments of the Farallon plate[20].

We conclude that flat slabs form through a combination of trench retreat, suction, and the inability of overthickened oceanic crust to sink below some depth (about 90 km) until sufficiently eclogitized to become negatively buoyant once again. Flat slabs that extend laterally beyond some critical distance from the buoyant overthickened crust will begin to founder, even in the presence of other factors such as suction and trench retreat. The Peruvian flat slab provides insights into the temporal evolution of flat slabs from initial shallowing to collapse, yielding new constraints for the reconstruction of flat-slab genesis and the nature of the flat-slab foundering.

Online Content Methods, along with any additional Extended Data display items and Source Data, are available in the online version of the paper; references unique to these sections appear only in the online paper.

Received 24 October 2014; accepted 28 May 2015.

1. Bedle, H. & van der Lee, S. Fossil flat-slab subduction beneath the Illinois basin, USA. *Tectonophysics* **424,** 53–68 (2006).
2. Humphreys, E. *et al.* How Laramide-age hydration of North American lithosphere by the Farallon slab controlled subsequent activity in the western United States. *Int. Geol. Rev.* **45,** 575–595 (2003).
3. Vogt, P. R. Subduction and aseismic ridges. *Nature* **241,** 189–191 (1973).
4. van Hunen, J., Van Den Berg, A. P. & Vlaar, N. J. On the role of subducting oceanic plateaus in the development of shallow flat subduction. *Tectonophysics* **352,** 317–333 (2002).
5. Manea, V. C., Pérez-Gussinyé, M. & Manea, M. Chilean flat slab subduction controlled by overriding plate thickness and trench rollback. *Geology* **40,** 35–38 (2012).
6. Gerya, T. V., Fossati, D., Cantieni, C. & Seward, D. Dynamic effects of aseismic ridge subduction: numerical modelling. *Eur. J. Mineral.* **21,** 649–661 (2009).
7. Skinner, S. M. & Clayton, R. W. The lack of correlation between flat slabs and bathymetric impactors in South America. *Earth Planet. Sci. Lett.* **371–372,** 1–5 (2013).
8. Rosenbaum, G. *et al.* Subduction of the Nazca Ridge and the Inca Plateau: insights into the formation of ore deposits in Peru. *Earth Planet. Sci. Lett.* **239,** 18–32 (2005).
9. Eakin, C. M. *et al.* Response of the mantle to flat slab evolution: insights from local S splitting beneath Peru. *J. Geophys. Res.* **41,** 3438–3446 (2014).
10. Ward, K. M. *et al.* Ambient noise tomography across the Central Andes. *Geophys. J. Int.* **194,** 1559–1573 (2013).
11. Phillips, K. & Clayton, R. W. Structure of the subduction transition region from seismic array data in southern Peru. *Geophys. J. Int.* **196,** 1889–1905 (2014).
12. Cahill, T., & Isacks, B. L. Seismicity and shape of the subducted Nazca plate. *J. Geophys. Res.* **97,** 17503–17529 (1992).
13. Hayes, G. P., Wald, D. J., & Johnson, R. L. Slab 1.0: a three-dimensional model of global subduction zone geometries. *J. Geophys. Res.* **117,** B01302 (2012).
14. Hasegawa, A., & Sacks, I. S. Subduction of the Nazca plate beneath Peru as determined from seismic observations. *J. Geophys. Res.* **6,** 4971–4980 (1981).
15. Uyeda, S., Watanabe, T., Ozasayama, Y. & Ibaragi, K. Report of heat flow measurements in Peru and Ecuador. *Bull. Earthquake Res. Inst.* **55,** 55–74 (1980).
16. Arrial, P. A. & Billen, M. I. Influence of geometry and eclogitization on oceanic plateau subduction. *Earth Planet. Sci. Lett.* **363,** 34–43 (2013).
17. International Seismological Centre. *On-line Bulletin* (ISC, http://www.isc.ac.uk (2012).
18. Liu, L. *et al.* The role of oceanic plateau subduction in the Laramide orogeny. *Nature Geosci.* **3,** 353–357 (2010).
19. Jones, C. H., Farmer, G. L., Sageman, B. & Zhong, S. Hydrodynamic mechanism for the Laramide orogeny. *Geosphere* **7,** 183–201 (2011).
20. Sigloch, K., McQuarrie, N. & Nolet, G. Two-stage subduction history under North America inferred from multiple-frequency tomography. *Nature Geosci.* **1,** 458–462 (2008).
21. Gripp, A. E. & Gordon, R. G. Young tracks of hotspots and current plate velocities. *Geophys. J. Int.* **150,** 321–361 (2002).
22. Instituto Geológico Minero y Metalúrgico. On-line catalog. (INGEMMET, http://www.ingemmet.gob.pe (2014).

Supplementary Information is available in the online version of the paper.

Acknowledgements We thank R. Clayton and P. Davies for providing the records from eight PERUSE stations. The PULSE experiment was supported by NSF grants EAR-0944184 (to L.S.W.), EAR-0943991 (to S.L.B.) and EAR-0943962 (to M.D.L.). The CAUGHT project was supported by NSF grants EAR-0908777 (to L.S.W.) and EAR-0907880 (to S.L.B.).

Author Contributions S.K.A. generated the tomographic model. L.S.W. developed the model of temporal evolution. A.K. provided earthquake locations. S.K.A, L.S.W. and A.K. developed the ideas and wrote the paper. S.L.B., M.D.L., G.Z., H.T. and C.C. contributed to data collection and paper editing.

Author Information Reprints and permissions information is available at www.nature.com/reprints. The authors declare no competing financial interests. Readers are welcome to comment on the online version of the paper. Correspondence and requests for materials should be addressed to S.K.A. (sknezevi@live.unc.edu).